International Conference on Space Optics—ICSO 2018

Chania, Greece

9–12 October 2018

Edited by Zoran Sodnik, Nikos Karafolas, and Bruno Cugny

HgCdTe APDs detector developments at CEA/Leti for atmospheric lidar and free space optical communications

Johan Rothman

Pierre Bleuet

Julie Abergel

Sylvain Gout

et al.

International Conference on Space Optics — ICSO 2018, edited by Zoran Sodnik, Nikos Karafolas, Bruno Cugny, Proc. of SPIE Vol. 11180, 111803S · © 2018 ESA and CNES · CCC code: 0277-786X/18/$18 · doi: 10.1117/12.2536055

HgCdTe APDs detector developments at CEA/Leti for atmospheric LIDAR and Free space optical communications

Johan Rothman*[a], Pierre Bleuet[a], Julie Abergel[a], Sylvain Gout[a], Gilles Lasfargues[a], Lydie Mathieu[a], Jean-Alain Nicolas[a], Jean-Pierre Rostaing[a], Stephanie Huet[a], Pierre Castelein[a], Kévin Aubaret[b], Olivier Saint-Pé[b]
[a]Univ. Grenoble Alpes, CEA, Leti, MINATEC Campus, 17 rue des Martyrs, 38054 Grenoble, France; [b]Airbus Defense and Space SAS, 31 rue des Cosmonautes, ZI du Plays, 31402 Toulouse

ABSTRACT

HgCdTe APD detector modules telecommunication are developed at CEA/Leti for atmospheric LIDAR and free space optical (FSO). The development is driven by the design and manufacture of generic sub-assemblies that can be adapted in each detector module to meet the specific detector requirements of each application. The optimization of such sub-assemblies is detailed in perspective of the challenges that are set by the specifications for detector modules currently developed for atmospheric LIDAR, in the scope of an R&T CNES project for Airbus and an H2020 project HOLDON, and FSO, in the scope of an ESA project and in collaboration with Mynaric Lasercom GmbH. Two detector modules have recently been delivered to Airbus DS for extensive LIDAR simulation tests. Initial characterization of these modules shows that the input noise, NEP=10-15fW/√Hz (5 photons rms) have been reduced by a factor three compared to previously developed large area detectors although the bandwidth have been increased to 180 MHz in order to respond to the requirements of high spatial depth resolution. The temporal remanence was 10^{-4} at 200 ns after the detection of short light impulse, which is compatible with demanding LIDAR applications such as bathymetric profiling.

Keywords: HgCdTe, APD, Free Space Optical communication, atmospheric LIDAR

1. INTRODUCTION

HgCdTe APDs have opened a new horizon in photon starved applications due to their exceptional performance in terms of high linear gain, low excess noise and high quantum efficiency. Both focal plane arrays (FPAs) and large area single element using HgCdTe APDs have been developed to detect without signal degradation the spatial and/or temporal information contained in photon fluxes with a low number of photon in each spatio-temporal bin. The enhancement in performance that can be achieved with HgCdTe has subsequently been demonstrated in a wide scope of applications such as astronomical observations, active imaging, deep space telecommunications, atmospheric LIDAR and mid-IR (MIR) time resolved photoluminescence measurements using detectors manufactured at CEA/Leti [1]-[6], DRS Leonardo [7]-[10] and Leonardo [11], [12].

The present communication focus on the present development and tests of detector modules at CEA/Leti for applications that only require temporal information and can be addressed with a single or a few APDs, such as atmospheric LIDAR and free-space optical communication (FSO). The detectors are made of components and sub-assemblies, including the HgCdTe APDs, which are developed and/or adapted for each application in order to comply with their specific requirements. These sub-assemblies are described in the next section together with the status and objectives for our current detector module development for FSO and atmospheric LIDAR. In the thereafter following section 3, we report characterization results on a detector developed for high depth resolution atmospheric LIDAR, in collaboration with Airbus DS in the scope of an R&T CNES project. Section 4 present a summary and the perspectives for time resolved HgCdTe APDs detector modules at CEA/Leti.

*johan.rothman@cea.fr; phone +33 4 38 78 21 67 ; fax +33 4 38 78 51 67; www.leti-cea.fr

2. HGCDTE APD DETECTOR DEVELOPMENT AT CEA LETI

2.1 Detector modules

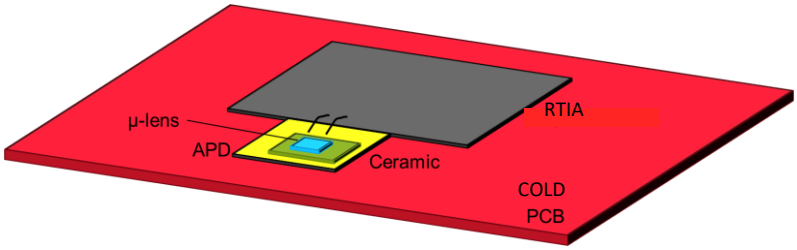

Figure 1. Cold PCB sub-assembly based on a deported resistive trans-impedance amplifier RTIA which is wire bonded to the HgCdTe APD-ceramic IC hybrid. Micro-lenses is optionally fabricated into the backside CZT substrate of the HgCdTe die.

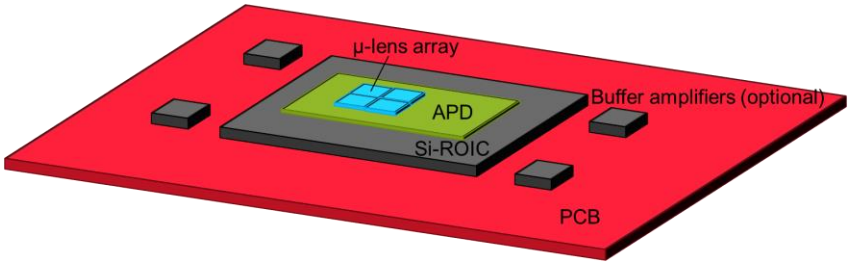

Figure 2.Cold PCB sub-assembly based on a high sensitive HgCdTe APD-ROIC. Optional buffer amplifiers can be used to amplify on the PCB.

The detector modules that are developed at CEA/Leti are constituted of sub-assemblies that are designed and/or adapted to meet the requirements for each applications in terms of operating temperature, bandwidth, active area, optical coupling, electrical interface and cooling system:

- **HgCdTe APDs:** The HgCdTe APDs are designed and manufactured at CEA/Leti in epitaxial layers that are grown in house using liquid phase epitaxy (LPE) or molecular beam epitaxy (MBE). This is the most critical part of the detector module as it is the high gain in HgCdTe APDs with a close to negligible loss in information measured by the photon noise limited signal to noise ratio which is the main motivation for using this technology. The geometry of the APDs needs to be adapted to meet the requirements in terms of BW, gain, operating temperature and active area. The physics and limitation of HgCdTe APDs have recently been detailed in references [13].
- **Inter-connection (IC) network:** CEA/Leti HgCdTe APDs are made in a planar n/p geometry [13] and needs to be used with backside illumination in order to benefit from a high quantum efficiency (QE) and low excess noise avalanche gain (F). At present, the IC-hybrids are also used to form large area detector by interconnecting small area APDs separated by a pitch of 10 to 30 μm.
- **Pre-amplifier**: The small amount of charges that are generated in the APD must be collected by an amplifying circuit which translates the detected charges or charge flow to a usable electric voltage signal which can be sampled outside the detector module. We are presently using two approaches to collect the signal from the APD. In the first approach, illustrated in figure 1, the pre-amplifier is deported close to an APD-IC hybrid. The APD is connected to the pre-amplifier using wire bonding techniques. This approach has the advantage to be versatile as the APD characteristics and choice of pre-amplifier can be adapted to the requirements of each application. It is also possible to use commercially available amplifiers which is in favor of reduced development costs and facilitates the development of detectors with bandwidths above 1 GHz. The main

drawback of this approach is the large input capacitance of the amplifier that makes it difficult to reach noise levels compatible with single photon detection for typically useful APD gains of 100. To reach this ultimate sensitivity and/or to optimize the functionalities of the pre-amplifier it is therefore convenient to design dedicated read-out integrated circuits (ROIC) onto which the APDs can be directly hybridized. The direct hybridization allows to minimize the input capacitance of the amplifier and the approach has been used to demonstrate single photon detection with APD-ROIC hybrids developed by CEA/Leti[14], DRS [8]and Raytheon [15]. The APD-ROIC hybrid configuration is schematically illustrated in figure 2.

- **Micro-lenses:** A process have been developed to form micro-lenses into the high index CdZnTe (CZT) substrate used to grow the epitaxial layer. The micro lens is centered on the active APD area, as is illustrated in figure 3a). The use of micro lenses allows to reduce the active APD area which is in favor of lower dark current and/or higher operating temperature and lower diode capacitance. The latter is crucial to reduce the diode capacitance which can limit the bandwidth of the APD and pre-amplifier and increase the noise of the pre-amplifier. The micro-lens capability was developed within the frame of an R&T CNES project that aimed to optimize the optical coupling for FSO and atmospheric LIDAR applications. Figure 3b) and 3c) shows a 200 µm micro lens patterned into the CZT substrate and an intensity map obtained through the focusing onto a 10 µm pitch FPA with a lens having a focal length of 700 µm. The obtained spot of 60 µm correspond to the expected size for incident light with a field of view of 14 °.
- **(Cold) Printed Circuit Board (PCB):** A PCB is used to connect the bias supplies to the APD and the pre-amplifier circuits. This board can also support additional buffer amplifiers, temperature probes and passive components that are used to filter the bias supplies.
- **Packaging:** To reach a high useful gain at low reverse bias, the bandgap of the HgCdTe material used to manufacture the APDs needs to be below 0.5 eV. This implies that the APD active area, dark current and operating temperature needs to be carefully evaluated to avoid a limitation in sensitivity due to the noise associated with the dark current generation in the APD. In application that requires a large active area and a low bandwidth it is mandatory to cool the detectors below room temperature. Two approaches have been used at CEA/Leti at present. The first detectors were cooled using a 4-stage thermos-electric cooler (TEC) in a vacuum package. A first prototype using such a packaging is pictured in figure 4a). This approach allowed us to reach an operating temperature of 190 K and enabled to demonstrate (deported) amplifier noise limited performance for large area APDs (diameter ~200 µm) in the order of 0.13 to 0.6 nW for detectors modules with bandwidth of 20 and 80 MHz (NEPh better), respectively [2], [3]. To reach higher sensitivities at equivalent bandwidth, down to single photon detection, it is mandatory to reduce the noise using a ROIC, increase the APD gain, use a cold filter to reduce background flux on the detector and/or reduce the operating temperature. A low operating packaging solution have been developed based on a liquid nitrogen cryostat, manufactured by KADEL engineering and pictured in figure 4b). This cryostat offers a versatile solution for laboratory application demonstrations with detectors for down to single photo detection capability. For applications that requires very high bandwidth, it is possible to operate the HgCdTe APDs at room temperature without cooling. This is expected to be the case for the 10 GHz detector developed for Mynaric Lasercom GmbH, in which case we will not develop a dedicated packaging.
- **Proximity electronics:** Electronic boards are favorably used in close proximity to the packaging in order to supply low noise biases and to sample the output signal and to simplify the use of the detection modules. At present, we have developed a generic proximity electronics board that provides 20 low noise buffered bias supplies which are set by individual DACs that are controlled through a microcontroler (MCP2210 from Microchip) via a USB interface. The developed proximity electronics board can be seen at the backside of the LN2 cryostat in figure 4b).

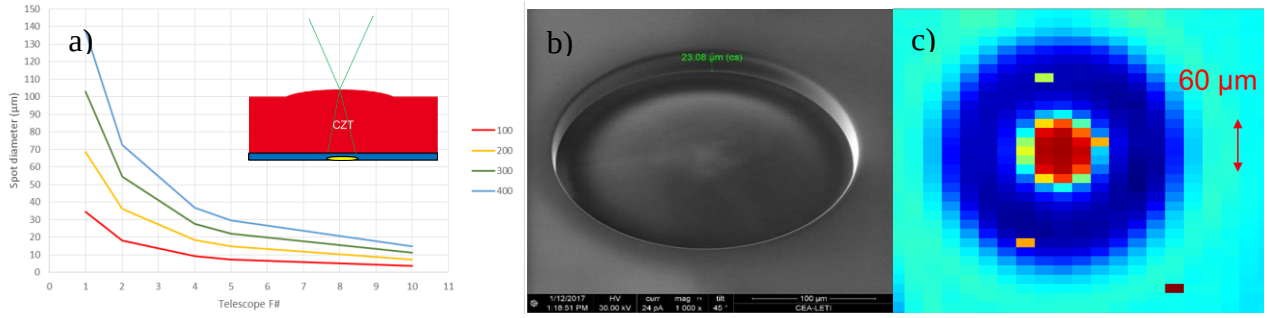

Figure 3. a) Schematic illustration of a micro lens fabricated in the backside CZT substrate of the detector with the APD at the focal distance of the lens and the corresponding spot size as a function of the F# of the collecting optics, b) scanning electron micrograph of a 200 µm diameter micro-lens made in a CZT substrate and c) Signal distribution in and around a micro-lens fabricated with a focal distance of 700 µm into the CZT substrate of 10 µm HgCdTe FPA illuminated at a flat field with a field of view FOV=14 ° (F#=4). The spot size is equal the expected value.

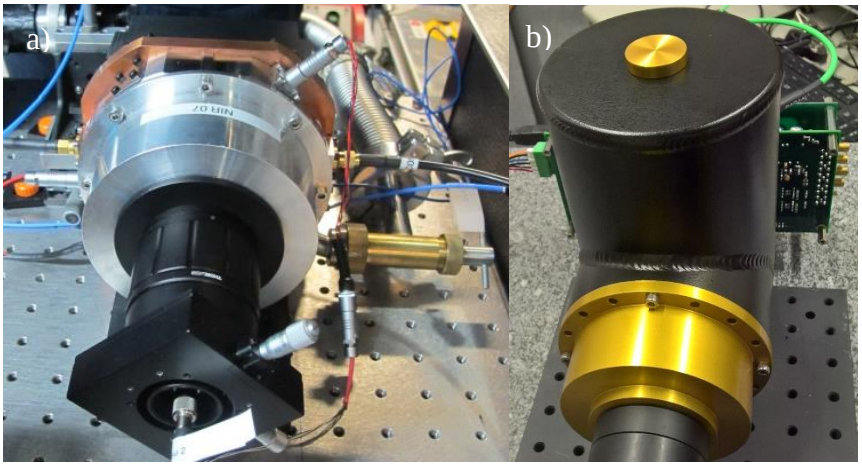

Figure 4. a) TEC cooled detector package used during the LLCD demonstration and b) LN2 cryostat and proximity electronics used for high sensitivity LIDAR and FSO.

2.2 Detectors for FSO

FSO is a typically photon starved application in which the number of detected photons per bit is limited by the combination of low emitted laser power, beam divergence and possible atmospheric absorption. A first HgCdTe APDs detector module was developed at CEA/Leti for deep space telecommunications. Characterized by a bandwidth of 80 MHz and a NEP=65fW/√Hz (BW= 80 MHz), it was successfully used to demonstrate 80 Mbps rate from moon to earth during the LLCD experiment, in collaboration with ESA and NASA [1],[2]. This demonstration has spurred the interest for HgCdTe APDs for this application and we are presently developing two new detector modules for high sensitivity deep space FSA, with ESA, and for high 10 Gbps communication closer to earth in collaboration with Mynaric Lasercom GmbH.

The ESA project objective is to develop a 4 quadrant detector for deep space FSO applications, with single photon sensitivity and a bandwidth of 300 MHz on each detector. To reach single photon resolution, the detector is made using APD-ROIC hybrid integrated into a LN2 cryostat. An optical active area of 200 µm will be achieved using 4 quadrant micro lenses fabricated into the CZT substrate. At APD gains in excess of 100, the detector module should be capable of linear mode single photon detection. The bandwidth of the detector module is limited to 300 MHz by the Si ROIC. A hetero-structure APD architecture have been designed and is grown using MBE to optimize the quantum efficiency while minimizing the timing jitter at single photon level to a value below 100 ps. The expected performance of the detector is resumed in table 1. This sensitivity, high bandwidth and low jitter will not only be an asset for deep space FSO, but also for quantum optical applications such a Quantum Key Distribution (QKD) and we intend to develop a fiber coupled version of the detector. By distributing the signal on the 4 detectors, we expect to be able to detect single photons at GHz rates.

The detector for fast 10 Gbps FSO is developed in collaboration with Mynaric Lasercom Gmbh. The focus of this development is the optimization of the response time of the APDs to reach a bandwidth in the order of 10 GHz. A specific MBE grown hetero-structure –have been designed in this purpose, which should also limit the dark current generation to achieve room temperature operation. The high bandwidth and operating temperature requirement do also imply that the APD active area needs to be limited. Again, micro-lenses made in the CZT substrate will be used to reduce the active APD diameter while complying with the application requirements in terms of collection efficiency. The APD will be connected to a deported commercial TIA. No specific packaging will be used for this detector as the APD will be operated close to room temperature. The expected performance for this detector is resumed in table 1.

Table 1. Expected characteristics of the HgCdTe APD detector modules under development for FSO at CEA/Leti.

Specification	ESA deep space detector	Mynaric Lasercom 10 Gbps
Geometry	4 Quadrant	Single pixel
Quantum efficiency (QE)	80 %	80 %
Quantum efficiency to excess noise Factor Ratio (QEFR)	67 %	67 %
BW (Hz)	300 MHz	10 GHz
Jitter (ps)	<100 ps	10 ps
Optically Active area diameter	200 µm	50 µm
NEP (λ=1.55 µm)	<1.6 fW/√Hz	100 f W/√Hz
NEPh (photons rms)	<0.3	4

2.3 Detectors for atmospheric LIDAR

A first APD detector module was developed to respond the needs of Differential Absorption Lidar (DIAL) specified by Laboratoire de Méterologie Dynamique (LMD) within the scope of a CNES R&T project. The detector uses a deported RTIA and was cooled in a vacuum package using a 4-stage TEC. The characteristics of the detector and first CO2 DIAL measurements at LMD have been reported in references [3]-[4]. The first DIAL measurement showed that the use of HgCdTe APDs for direct detection LIDAR was in favor of increased range and higher temporal resolution, but also that a further increased sensitivity is needed to increase the range. In addition, a long term remanence was observed when the light was strongly absorbed by the atmospheric CO2, which impeded a correct extraction of the optical thickness at larger distances [4]. Large area APDs from the same batch were also submitted to proton irradiation and endurances tests that showed on a stable performance and motivated the pursuit of the development of large area HgCdTe APDs for applications in space [3].

Lidar detectors for atmospheric LIDAR are currently developed within the scope of R&T CNES projects and a H2020 project termed HOLDON. The aim of these projects is to optimize characteristics of the HgCdTe APD detector modules to comply the specific challenges imposed by atmospheric LIDAR measurements in terms of dynamic range, response time, temporal lag (remanence) and background noise. A new detector module has been developed within the scope of a CNES R&T project in collaboration with Airbus DS, aiming to meet specifications atmospheric and bathymetric profiling with high spatial depth resolution. This specification requires an increased bandwidth of the APD and the RTIA. The APD bandwidth has been increased by reducing the collection time of the photo-generated carriers by forming a macro-diode on specifically developed ceramic IC using HgCdTe with 15 µm pitch to form the large area APD. APD-IC hybrids are mounted onto a specifically designed cold PCB, illustrated in figure 5, and connected by wire bonding to two different deported RTIA. The first amplifier is a ROIC that was developed at CEA/Leti with an expected bandwidth of 100 MHz and a noise below 1 pA/√Hz, termed CL MEATS [16]. This amplifier was designed to be used with a direct hybridization with a 5x5 array at a pitch of 30 µm. This pitch do not allow to meet the BW specification with the available design of APDs. For this reason, the amplifier was used in a deported mode in which the performance of the ROIC could be degraded due to the additional capacitance at the input of the amplifier. A second commercial

RTIA (C-RTIA), with a nominal bandwidth of 200 MHz and an expected noise of 3 pA/√Hz was therefore implanted as a back-up on the cold PCB. The cold PCB with amplifier and APD-IC hybrid, mounted on the cold post of the LN2 cryostat, is illustrated in figure 5. Two detector modules have been developed and delivered to Airbus DS for characterization on a specifically LIDAR simulation test bench at λ=1.06 µm. First characterization results obtained from measurements at CEA/Leti and Airbus are reported in section 3.

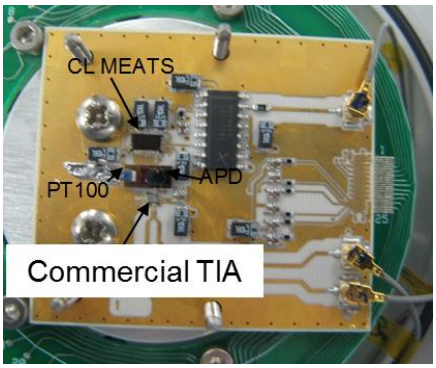

Figure 5. Cold PCB used to connect the APD-IC hybrid with the CL MEATS and C-RTIA amplifier in the high depth resolution LIDAR detection module.

The aim of the HOLDON project, which started in beginning of 2018, is to develop a versatile detection chain that shall meet most of the application requirements for atmospheric LIDAR measurements. The main tasks and partners of the project are:

- Detector development
  - *CEA/Leti (France):* HgCdTe APDs, Si ROIC design
- Proximity electronics and test equipment
  - *IDQuantique (Switzerland):* Proximity electronics and signal sampling, cryo-coolers for flight modules
  - *Alter (Spain) :* uv to NIR LIDAR signal generator
- LIDAR application demonstration
  - *DLR (Germany):* CH_4, CO_2 IPDA
  - *LMD (France):* CO_2 DIAL
  - *AIRBUS DS (France):* Wind, atmospheric profiling, bathymetry
- Project management
  - *Absiskey (France)*

The project objective and logic is illustrated in figure 6. LIDAR application requirements in fields varying from greenhouse gas detection (CO_2 DIAL at LMD, CH_4 IPDA at DLR), and cloud and aerosol profiling (at Airbus DS, using a LIDAR simulator from uv to NIR developed by ALTER) have been used to define the detector specifications. The detection chain is constituted of an HgCdTe APD-ROIC (developed at CEA/Leti) that will be integrated into low operating temperature packages (LN2 cryostat and sterling cooler). Specific proximity electronics will be developed by IDQ to control the functionalities of the detector and to sample the data. The main technical objective is to obtain a dynamic range, of 6 order of magnitude, while achieving photon shot noise limited detection for signals down to 1 photon per laser shot and observation time. The HOLDON approach to meet these extreme specifications is to use a Si-CMOS ROIC in which the gain and temporal resolution is adapted during duration of the return signal with the goal to enable a photon noise limited detection over the signals full dynamic range. This functionality is expected be met by implementing a dual mode of operation: a real-time trans-impedance mode will be used to sample the signal outside the cryostat on a proximity electronics card. This mode is adapted to the higher end of the dynamic range. The other mode is what is termed on-chip sampling mode (OCS), in which the signal will be sampled in a number of analog temporal bins

in the ROIC and that will be read out at a lower speed. The OCS mode will in particular be used to address the lower end of the dynamic range.

In addition to the development of the dedicated ROIC, dedicated HgCdTe APDs will be processed during HOLDON in order to optimize the quantum efficiency at the expected laser wavelengths, maximize the APD gain, reduce the excess noise factor and reduce the temporal remanence. Micro-lenses will also be explored to reduce the APD area in favor of lower dark currents and diode capacitance. The objective in performance of the HOLDON detector is compared to the other CEA/Leti LIDAR detection modules in table 2, illustrating the expected increase in performance on all parameters.

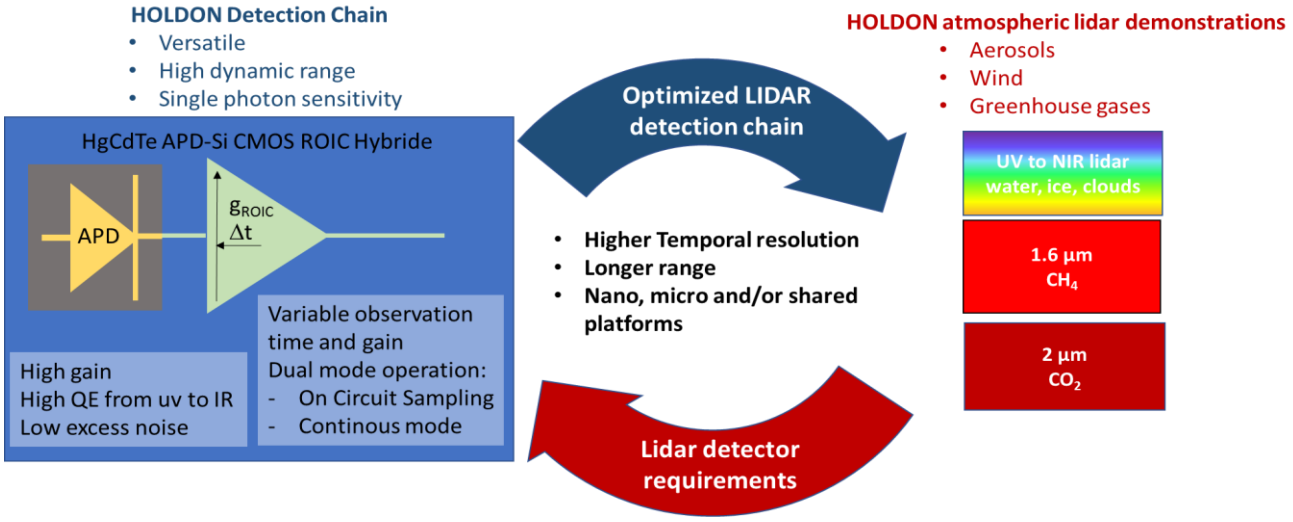

Figure 6. Schematic illustration of the detection chain concept and work logic horizon 2020 project HOLDON.

Table 2. Expected characteristics of the HgCdTe APD detector modules under development for atmospheric LIDAR at CEA/Leti.

Specification	LMD detector	Airbus detector Objective	HOLDON Objective
Excess noise factor F	1.3	1.3	1.2
Quantum efficiency (QE)	80%	80 %	90%
Quantum efficiency to excess noise Factor Ratio (QEFR)	62%	62 %	75%
Bandwidth	20 MHz	*>100 MHz*	
Remanence at t > 5/BWAPD	$1x10^{-4}$	$<1x10^{-4}$ after 100 ns	$1x10^{-5}$
Temporal resolution	25-50 ns	10 ns	5 to 10 000 ns
Photon Noise Limited Dynamic Range (PNDR)	33 dB		60 dB (10^{6}-10^{12} p/s)
Spectral Range	0.8 to 3 µm	0.8 to 3.3 µm	0.3 to 3 µm
Detector noise	40 photons	*<40 photons*	<1 photon
Minimum detected photon noise limited signal (photons/TC)	1600 photons		<1 photon
Active Detector diameter	200 µm	*>150 µm*	To be reduced using µ lenses

3. HIGH BANDWIDTH LIDAR DETECTOR MODULE CHARACTERIZATION

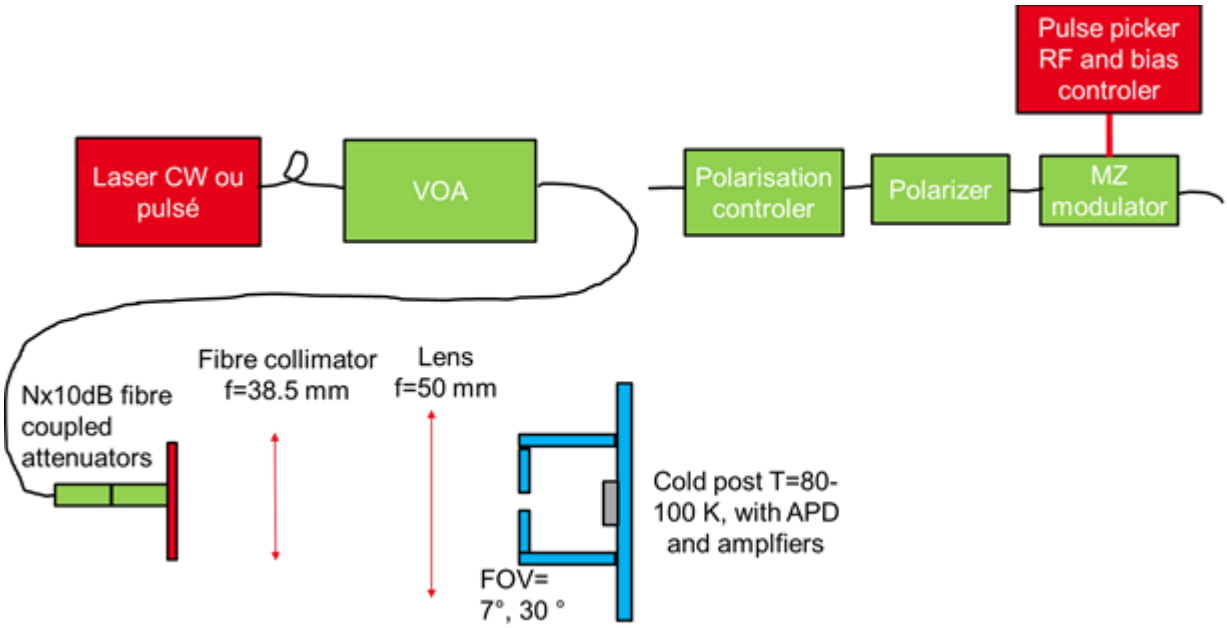

Figure 7. Illustration of the experimental set-up used CEA/Leti to characterize the responsivity, sensitivity (NEP), information conservation QEFR and remanence.

Detection modules for high depth resolution atmospheric profiling have been developed in collaboration with Airbus DS in the frame of an R&T CNES project, as described in section 2.2. The experimental set-up used to characterize the detector modules is illustrated in figure 7. The detector responsivity, noise equivalent power (NEP), and quantum efficiency to excess noise ratio measured by focusing a CW laser on the HgCdTe APD. The incident optical power, P_{opt}, is estimated using a fiber coupled Variable Optical Attenuator (VOA) and a variable number of fixed 10 dB fiber coupled attenuators. The external responsivity of the detector is directly estimated from ratio of the voltage difference between induced by the laser ΔV_{laser} and P_{opt}:

$$R = \frac{\Delta V_{laser}}{P_{opt}} \tag{1}$$

The noise equivalent input power density, NEP, and noise equivalent number of photons, NEPh, are estimated from the noise standard deviation without incident light:

$$NEP = \frac{\sigma_V}{R\sqrt{BW}} \tag{2}$$

$$NEPh = \frac{\sigma_V}{R}\frac{TC}{h\nu} = \frac{\sigma_V}{R}\frac{1}{h\nu 2BW} \tag{3}$$

Where TC is the characteristic time over which the photo current is integrated at given bandwidth, BW, limited by the detector and/or by applying a low pass filter on the sampled signal. In the figure 8 we report the measured responsivities and NEP values at the output of the C-RTIA and CL MEATS detection chains. The bandwidth was limited by numerical filtering on the sampled signals in order to control the BW over which the noise is integrated and to limit the integration of amplifier noise at higher frequencies where the spectral noise density tends to peak. The increase in gain in the HgCdTe APDs results in a strong increase in responsivity and a reduced NEP up to a reverse bias in the order of -12 V. The corresponding APD gain at -12 V reverse bias was 300 and 170 for the C-RTIA and CL MEATS outputs, respectively. The difference in APD gain is due to a difference in bias on the input nodes of the TIA which can be estimated to be larger than 1 V. At the highest reverse bias we observe a NEP in the order of 10-15 fW/√Hz on both detectors, which corresponds to NEPh values of about 5 photons at 80 MHz, for the C-RTIA output, and 15 Photons at 8

MHz, for the CL MEATS output. In terms of NEP, these values are at least a factor 3 lower than what was observed for the TEC cooled detectors that were used for deep space FSO (see section 2.2) and DIAL (see section 2.3).
The information conservation in the detector due to the quantum efficiency (QE) and excess noise factor (F) of the APD, measured by the ratio QEFR=QE/F, can be directly estimated from the degradation of the signal to noise ratio with respect to the photon noise limited CW signal at the input with a power P_{opt} :

$$QEFR = \frac{SNR_{out}}{SNR_{in}} = \frac{\left[\frac{\Delta V_{laser}}{\sigma_{\Delta V_{laser}}}\right]^2}{\left[\frac{P_{opt}}{h\nu}\frac{1}{2BW}\right]} \quad (4)$$

The value of QEFR was found to decrease when higher BW where used to integrate the noise. This dependency indicates a variation in gain between high and low frequencies. An intermediate bandwidth of 80 MHz where used to estimate the QEFR on the C-RTIA detection chain yielding an external fiber to detector QEFR=51 %. This value was obtained without AR coating and could also be reduced be an optical coupling losses due to multiple optical interface and the use of small field of view in the cold screen which could cause vignetting in case the optical axe is not well aligned with the APD active area.

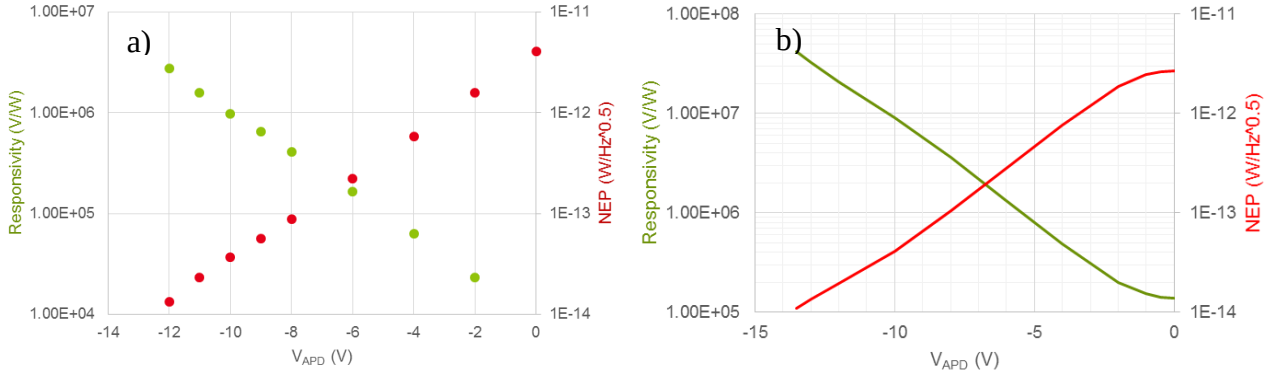

Figure 8. Variation of the responsivity and noise equivalent input power spectral density (NEP) as a function of the reverse bias of the a) C-RTIA output and b) CL MEATS output.

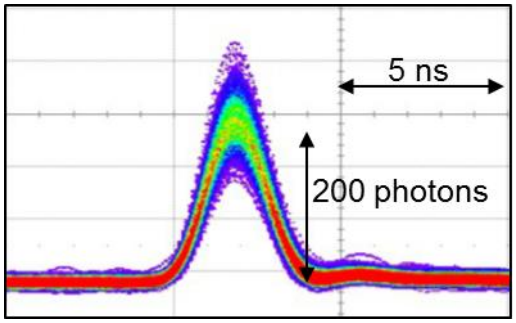

Figure 9. Impulse response of the C-RTIA channel at -12 V reverse bias.

The unfiltered bandwidth of each output was estimated from Fourier analysis of the impulse response of the detection module. The typical impulse response of the C-RTIA detection chain is illustrated in figure 9 for an average signal of about 200 photons, at which the photon shot noise gives a dominating contribution to the signal amplitude. The width at half maximum is FWHM=2.1 ns and the corresponding total bandwidth was estimated to 180 MHz, which comply with the Airbus specifications for atmospheric profiling. Similar measurements were performed on the CL MEATS detection chain and showed on a total bandwidth of about 20 MHz (FWHM of 33 ns). This is below the expected bandwidth of this amplifier and the reduction in bandwidth is probably due an excess input capacitance when using the ROIC as a deported amplifier. The limited bandwidth do not comply with the Airbus DS specification which is why this detection chain is more adapted for DIAL or IPDA measurements with reduced depth resolution.

The linearity of the detector modules was estimated using pulsed measurements and by attenuating the signal using the VOA. The use of a variable attenuator is associated with an uncertainty on the value of attenuation of a few percent and is not accurate enough to verify linearity down to 10^{-3} level which tend to be required for the most demanding lidar applications. A first linearity measurement with the C-RTIA detection chain is reported in figure 10. The detector is found to linear over close to 3 order of magnitudes but tend to saturate when the output signal approaches 100 mV. This saturation can be caused by the use of the C-RTIA at low temperatures and/or the saturation of a pre-amplifier which was not used in ideal conditions during this measurement. We are currently developing a new measurement technique based on the ratio of two consecutive pulses with constant power ratio to be able to probe the linearity with high precision over more than 6 orders of magnitudes. To reduce uncertainty, a complementary measurement is also being set-up at Airbus DS, with an integrated sphere and a calibrated radiometer.

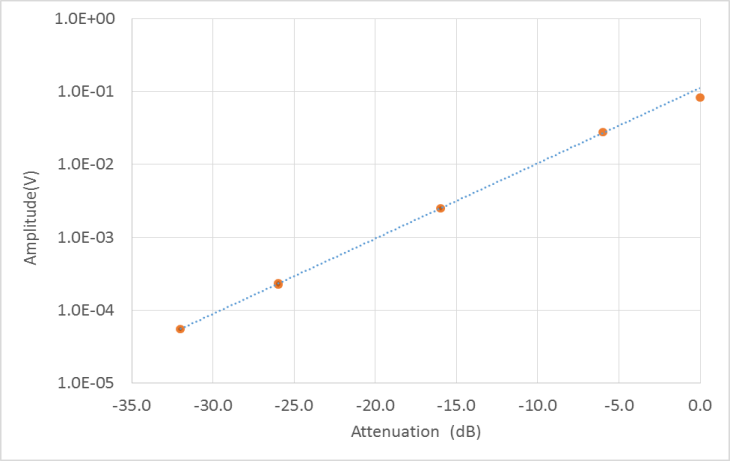

Figure 10. Signal variation as a function of optical attenuation measured on the C-RTIA channel.

Remanence is a trailing signal that is observed on time scales longer than the linear response time of the detector that can interfere with atmospheric LIDAR signals, which can evolve over 5-6 orders of magnitudes. Such interference was for example observed during the CO2 DIAL measurements on a time scale of 10 µs after the detection of long duration high intensity peak. In atmospheric or bathymetric LIDAR that is developed at AIRBUS DS, the required depth resolution is one meter, which corresponds a time scale of 10 ns during which the detector should ideally relax. Remanence measurement was carried out at CEA/Leti using the set-up illustrated on the right hand side of figure 7. The goal of the set-up is to use a Mach-Zehnder fiber-coupled light modulator to increase the extinction ratio of an initially pulsed laser source to guarantee that no laser light is incident on the APD after the detection of the laser pulse. The polarization of the pulsed laser light was aligned with an in-line fiber optic polarizer that blocks orthogonal polarized light, which is not subject to modulation by the Mach-Zenhder modulator, by at least 23 dB. The axe of the light from the output of the polarizer is aligned with the axe of the Mach-Zehnder modulator in order to generate an extinction ratio of at least 30 dB. Given an initial extinction ratio of at least 30 dB of the pulsed laser, we expect the extinction ratio of the light on the detection to be higher than 50 dB (10^{-5}) at 5 ns from the detection of the pulse. Hence, the measured remanence is dominated by long term relaxation that originates from the HgCdTe APD, RTIA amplifier and/or sampling electronics.
Figure 11 reports the measured impulse response on the C-RTIA output signal, which was pre-amplified using a differential instrumental amplifier and sampled with an 8 bit Lecroy oscilloscope using 3 bit ERES filtering and waveform averaging to increase the dynamics of the sampled signal to about 40 dB. The shape of the response in figure 11 shows on three contributions to the response time. The fastest contribution (I), observed over the first 10 ns, corresponds to the linear response time of the APD. A slower contribution (II) is consistent with a contribution from the collection of residual carriers through diffusion and is characterized by an exponential decay with a time constant equal to the expected life time of the minority carriers in the HgCdTe substrate of about 15 ns. This contribution can be strongly reduced by concentrating the light within the active area of the APD using, for example, micro-lenses. A slower trailing edge (III) is observed after 50 ns of the pulse detection and reaches a relative intensity below 10^{-4}, 200 ns after the main peak. At longer time scales, the signal is hidden in the residual noise. This contribution could origin from trapping in the APD and/or -relaxation phenomena in the amplifier or sampling electronics. Complementary measurement with different amplifier and sampling electronics needs to be made to separate the different contributions.

Such measurements will be performed at Airbus DS using the 1.06 µm LIDAR test bench and a high resolution 16 bit ADC.
The level of remanence observed in figure 11 is compared with an expected bathymetric LIDAR signal relative to the strong surface reflection peak for a standard and a more turbid scenario. It can be seen that the present detector is below the standard scenario but is likely to interfere with the more turbid case. Part of the remanence is due to the contribution (II) to the response and is likely to be reduced by concentrating the optical absorption within the active APD area. This optimization will be explored within the HOLDON project.
Two detector modules have been delivered to Airbus DS in view of extensive characterization on their λ=1.06 µm LIDAR simulation test bench. Initial characterization have been performed on the CL MEATS output and the first results are consistent with the results obtained at CEA/Leti. A complementary measurement at Airbus DS of the optically active area of the HgCdTe APD hybrid is reported in figure 12. The response is found to be homogeneous over the full area of the detector, with a small modulation between the APDs that are interconnected to from a large area APD of few percent. The variation in sensitivity is due to a reduced collection efficiency between the APDs. The observation of a small variation is consistent with the observation of a high QEFR value, but it can also be limited by the optical spot-size. Further characterization of both detection chains on this detector module are currently made at Airbus DS and will the subject of a future communication.
The results of the first characterizations are compared with the objectives in table 3. All characterized parameters are found to comply with the specifications except the QEFR value, which is reduced due to the absence of AR coating and a possible loss due to vignetting at the cold diaphragm, and remanence, which is a factor two above the specification at 100 ns. The remanence is partly limited by a slow response of carriers generated between the APDs in the macro pixel which is why a strong reduction can be expected by concentrating the light to the active APD area. This approach will be explored in the frame of the H2020 HOLDON project.

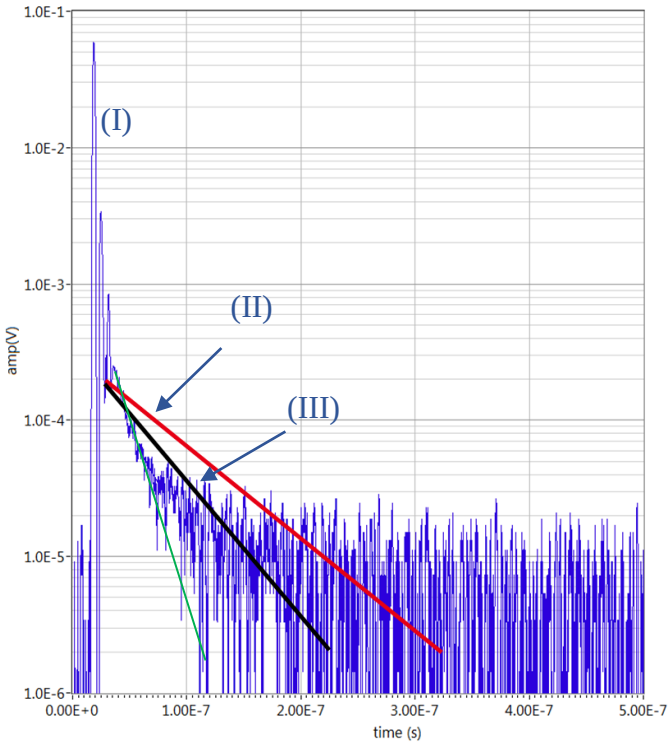

Figure 11. Short impulse remanence measurement on the C-RTIA output at-12 V reverse bias. The red and black lines corresponds to a backscattered bathymetric signal level with respect to the maximum intensity for a normal (red line) and a more turbid case (black line).

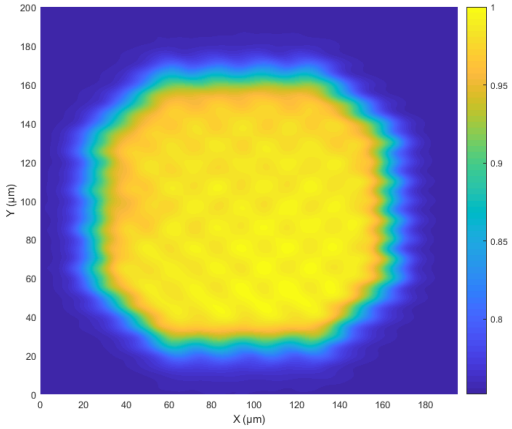

Figure 12. Spot-scan measurement on the CL-MEATS channel at – 5V detector reverse bias.

Table 3. Comparison between the nominal and obtained characteristics of the high depth resolution LIDAR HgCdTe APD detector module.

Specification	Airbus detector Objective	Airbus detector Results
Excess noise factor F	1.3	
Quantum efficiency (QE)	80 %	
Quantum efficiency to excess noise Factor Ratio (QEFR)	60 %	>50 % (No AR coating)
Bandwidth	*>100 MHz*	180 MHz
Remanence at t > 5/BWAPD	<1x10^{-4} after 100 ns	*1x10^{-4} after 200 ns*
Temporal resolution	10 ns	2 ns at full BW
Spectral Range	0.8 to 3.3 µm	0.8 to 3.3 µm
Detector noise	*<40 photons*	<5 photon
Minimum detected photon noise limited signal (photons/TC)	<1600	<25 photon
Active Detector diameter	*>150 µm*	140 to 160 µm

4. SUMMARY AND PERSPECTIVES

HgCdTe APD detector modules are developed at CEA/Leti for time resolved applications such as atmospheric LIDAR and FSO. After first demonstration with detector modules based on TEC cooled large area the development is presently dedicated to the development of detectors with higher sensitivities and/or faster response time through the optimization of the HgCdTe APDs, using MBE grown hetero-structures, of the optical coupling, using micro-lenses patterned into the CZT substrate, of the electrical pre-amplifier and/or of the cryogenic packaging. For FSO, detector are currently developed for deep space application for ESA, a 4 quadrant detector with down to single photon sensitivity and a bandwidth 300 MHz, and a detector for higher data rates, up to 10 Gbps, and that will be operated at room temperature is developed in collaboration with Mynaric Lasercom GmbH.

Two detectors modules are also developed for atmospheric LIDAR applications. A dual channel detector with two 150 µm diameter HgCdTe detectors have been developed for Airbus DS within the scope of an R&T CNES project. The two channels are using two different deported amplifiers with different characteristics in terms of gain, input noise, bandwidth and remanence. Sensitivities in the range of 10-15 fW/√Hz were observed for the two detectors, representing a gain in sensitivity by a factor 3 compared to the TEC cooled detectors. A bandwidth of 180 MHz was measured on the channel that used a commercial RTIA and did comply with the requirements for high depth resolution LIDAR. In addition, remanence measurement showed that this detector had a trailing relative signal of about 10^{-4}, 200 ns after the detection of an impulse, and could be compatible with the demanding requirements for bathymetric profiling. Further characterizations of this detector module are currently made at Airbus DS. The second detector module is developed within the H2020 project HOLDON with the objective to make a versatile full detection chain that will be capable of responding to needs of most LIDAR applications. The optimization of the HgCdTe APDs, ROIC and optical coupling should enable to reach a 60 dB photon noise limited dynamic range with down to single photon detection capability for observation times ranging from 10 ns to 10 µs.

ACKNOWLEDGEMENTS

The authors which to acknowledge CNES, ESA, Mynaric LaserCom AG and the European Commission's Horizon2020 program for supporting the development and optimization of time resolved HgCdTe APD detector modules. The HOLDON project has received funding from the European Union's Horizon 2020 research and innovation programme under grant agreement No 776390. You can visit our website http://holdon-h2020.eu/ and join our community on linkedIn "HOLDON project"

REFERENCES

[1] I. Zayer, et al., *SpaceOps 2014 Conference*, 1919 (2014)
[2] J. Rothman *et. al.*, Proc. SPIE, 9647, 96470N (2015)
[3] J. Rothman, G. Lasfargues, B. Delacourt, A. Dumas, F. Gibert, A. Bardoux, M. Boutillier, *CEAS Space J*. **9**, 507 (2017)
[4] A. Dumas, J. Rothman, F. Gibert, D. Édouart, G. Lasfargues, C. Cénac, F. Le Mounier, J. Pellegrino, J.-P. Zanatta, A. Bardoux, F. Tinto, and P. Flamant, *Applied Optics*, **56**, 7577 (2017)
[5] B. Delacourt, P. Ballet, F. Boulard, A. Ferron, L. Bonnefond, T. Pellerin, A. Kerlain, V. Destefanis and J. Rothman, *J. Electron. Mater*., **46**, 6817 (2017)
[6] A. Gassenq, L. Milord, J. Aubin, K. Guilloy, S. Tardif, N. Pauc, J. Rothman, A. Chelnokov, J. M. Hartmann, V. Reboud, and V. Calvo, *Appl. Phys. Lett.* **109**, 242107 (2016)
[7] X. Sun, J. B. Abshire, J. D. Beck, *Proc. SPIE*, **9114**, 91140K (2014)
[8] W. SullivanIII, J. D. Beck R. Scritchfield, M. Skokan, P. Mitra, X. Sun, J. Abshire, D. Carpenter, B. Lane, *J. Electron. Mater, 44, 3092 (2015)*
[9] P. F. McManamon, P. Banks, J. Beck, A. S. Huntington, E. A. Watson, *Proc. SPIE*, **9832**, 983202 (2016)
[10] X. Sun, J. B. Abshire, J. D. Beck, P. Mitra, K. Reiff, and G. Yang, *Optics Express*, **25**, 16589 (2017)
[11] Dani E. Atkinson, Donald N. B. Hall; Ian M. Baker; Sean B. Goebel; Shane M. Jacobson; Charles Lockhart; Eric A. Warmbier; *Proc. SPIE*, **9915**, 99150N (2016)
[12] G. Finger, I. Baker, M. Downing, D. Alvarez, D. Ives, L. Mehrgan, M. Meyer, J. Stegmeier, H. J. Weller, *Proc. SPIE*, **10563**, 1056311 (2017)
[13] J. Rothman, accepted for publication in *J. Electron. Mater.(2018), https://doi.org/10.1007/s1166*
[14] G. Vojetta, F. Guellec; L. Mathieu; K. Foubert; P. Feautrier; J. Rothman, *Proc. SPIE*,**8375**, 8375OY (2012)
[15] J. Asbrock, S. Bailey, D Baley, J. Boisvert, G. Chapman,G. Crawford, T. De Lyon, B. Drafahl, J. Edwards, E. Herrin, C. Hoyt, M. Jack, R.Kvaas, K. Liu, W. McKeag, R. Rajavel, V. Randall, S. Rengarajan and J.Riker., *Proc. SPIE*, **6940**, 69402O (2008)
[16] H. Amhaz, K. Foubert, F. Guellec and J. Rothman, "A novel 0.5GHz real time asynchronous photon detection and counting technique: ROIC design for cooled SWIR HgCdTe infrared detector," 2013 IEEE 11th International New Circuits and Systems Conference (NEWCAS), Paris, 2013, pp. 1-4